JOURNAL OF VIROLOGY, May 1985, p. 446–459
0022-538X/85/050446-14$02.00/0

Vol. 54, No. 2

Deletion in the 3′ *pol* Sequence Correlates with Aberration of RNA Expression in Certain Replication-Defective Avian Sarcoma Viruses

LU-HAI WANG

The Rockefeller University, New York, New York 10021

Received 21 December 1984/Accepted 4 February 1985

The RNA expression of a series of replication-defective recovered avian sarcoma viruses (rASVs) were studied. Abnormal-sized viral RNAs, both larger and smaller than the genome, were observed in the nonproducer cells infected with rASVs containing *env* and *pol* deletions. Each nonproducer clone contained a single provirus integrated at a unique site and expressed a unique RNA pattern. Upon rescuing of the sarcoma virus with a helper virus and subsequent cloning, the RNA pattern of individual nonproducer clones again displayed variation according to the integration sites. This was not seen in nondefective rASV or in rASVs containing only an *env* deletion. The aberrant RNA expression did not result from the lack of reverse transcriptase activity per se, since neither nonconditional nor temperature-sensitive mutants of RSV expressed abnormal viral RNAs in the absence of a functional reverse transcriptase. The abnormal RNA patterns could not be corrected in *trans* by helper virus functions. The unusual-sized RNAs in *env*$^-$ *pol*$^-$ rASV-infected cells are not due to splicing to alternative acceptor sites for *src* mRNA because there are no extra viral sequences between the 5′ leader and the *src* sequences; instead, they are due to the presence of extra sequences, most likely of cellular origin, at the 3′ ends of the viral RNAs. Based upon the extent of deletions in the viral genomes, the data suggest that deletion in the 3′ *pol* region of those rASVs results in a *cis* effect on the transcription and processing of the 3′ ends of viral RNAs. The unusual-sized viral RNAs are most likely due to read-through transcription from the right-hand terminus of provirus into downstream cellular sequences, followed by cleavage and polyadenylation at multiple sites of the 3′ region of the RNA transcripts. The extent of read-through transcription appears to depend on the chromosomal location of the provirus.

Gene expression can be controlled at the level of transcription, processing, and translation of mRNA (2, 7, 39, 58). Substantial knowledge regarding the consensus signal sequences for initiation, polyadenylation, and splicing of mRNA has been obtained from studies of molecularly cloned cellular genes and in particular from studies of viral genes (2, 7, 39, 58). Viral or cellular factor(s) and sequences other than those consensus signals that are likely to be involved in the control of transcription and processing of mRNA are largely unknown. Upon replication and integration of the retroviral genome, a complete transcriptional unit of provirus is formed as an integral part of the host cellular DNA. This system provides a model for studying mRNA transcription, not only the aspect of control by the viral sequences but also the effects of and the interaction with cellular sequences. Evidence for the effect of the neighboring cellular sequences on the expression of retroviral genomes has been documented (4, 5). Among other factors that may affect viral RNA transcription is methylation of the integrated provirus or its neighboring cellular DNA sequences, or both (3, 14, 26, 27, 35, 47).

Sequence analyses and in vitro transcription of retroviral DNAs have identified the presence of common control signals for transcription and processing of eucaryotic mRNA in the U3 region of the viral genome; these signals include the TATA box, CAT box, enhancer sequences, and AAUAAA sequence (11, 13, 28, 57). Study of the transcription of variant Rous sarcoma viral DNAs carrying deletions in the U3 region confirmed that the TATA box is essential for the precise initiation of transcription (13). Little is known about cellular or viral factor(s) that may be involved in the control of transcription or processing of retroviral RNAs, although one of the *gag* proteins, p19, of Rous sarcoma virus (RSV) has been suggested as playing a role in the regulation of RSV RNA processing (6, 30).

We recently reported that the recovered avian sarcoma viruses (rASVs) derived from a partial *src* deletion mutant of Schmidt-Ruppin RSV are all replication defective and contain various extents of deletions upstream from the newly regained *src* sequence (52). The purpose of this study was to analyze the RNA expression of those replication-defective rASVs. It was found that three independent isolates of rASVs carrying both *pol* and *env* deletions, but none of the rASVs with only an *env* deletion, displayed unusual patterns of viral RNAs in infected cells. These abnormal viral RNAs apparently resulted from read-through transcription from the provirus into cellular sequences, followed by cleavage and polyadenylation at multiple sites of the transcripts. These results suggest that certain *pol* sequences of RSV are involved in the control of transcription or processing of viral RNAs, or both.

MATERIALS AND METHODS

Cells and viruses. Chicken embryo fibroblasts (CEF) were prepared and maintained according to the published methods (15). Endogenous virus-negative (ev$^-$) (1) CEF that are susceptible to subgroup E virus infection (C/O type) were obtained from Celeste Simon and William Hayward of the Sloan-Kettering Cancer Research Institute. The viruses used in this study included Schmidt-Ruppin RSV, subgroup A (SR-A); a transformation-defective (td) mutant derived from it, td109, and the td109-derived recovered sarcoma viruses listed in Fig. 2 (52); an independent isolate of rASV, rASV1441 (56), which was derived from another td mutant, td108, of SR-A; two envelope-negative variants of RSV, Bryan high-titer (BH) RSV(−) (18) and SR NY8 (29); an

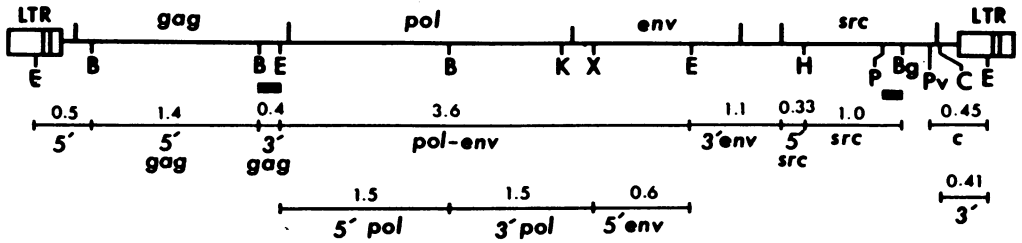

FIG. 1. Origin of DNA probes used for hybridization. The linear SR-A DNA is represented by the top horizontal line with one LTR at each end. The gene boundaries and restriction enzyme sites are shown above and below the line, respectively. The domain and the size in kb of individual DNA probes are shown below the SR-A genome. Two thickened bars below the 3' *gag* and the 3' *src* regions of the SR-A genome define the DNA fragments used in the RNase H digestion experiments. Abbreviations for restriction enzymes are as follows: B, *Bam*HI; Bg, *Bgl*I; C, *Cfo*I; E, *Eco*RI; H, *Hin*cII; K, *Kpn*I; P, *Pst*I; Pv, *Pvu*II; X, *Xho*I.

envelope-negative and polymerase-negative mutant of RSV, RSVα (17), two temperature-sensitive (ts) polymerase mutants, tsNY21 (44; C. E. Metroka, Ph.D. thesis, The Rockefeller University, New York, 1978), and tsLA337 (32); a ts mutant of group-specific antigen and polymerase tsNY45 (Metroka, Ph.D. thesis); and a subgroup E avian leukosis virus, RAV-60 (19).

Isolation of NP clones. Except for the original stock of td109-derived rASVs, all the defective sarcoma virus pseudotypes used in this study contained the helper virus RAV-1. Nonproducer (NP) clones of replication-defective ASV-infected CEF were prepared by isolating transformed colonies grown in semisolid agar medium containing antiserum against the helper virus according to the published method (21). Transformed colonies were picked 2 to 3 weeks later from plates infected with the highest dilution of viruses. After cells were dispersed from the picked colony by trypsinization, they were plated onto a 6-cm dish containing 10^6 normal CEF seeded 6 to 12 h previously. The cultures were overlaid with F10 medium containing 0.36% agar the next day and maintained at 41°C to promote the growth of transformed cells. Two to three days later the semisolid agar medium was replaced with F10 liquid medium, and the culture was shifted to 37°C. The culture of each NP clone was expanded to 3 to 16 10-cm plates for further biological and biochemical analyses. Overnight culture fluid was harvested at various stages of the culture and assayed by focus formation to check whether the infectious transforming viruses were released. Those remaining negative for producing transforming viruses after three to four transfers were judged as NP clones. If necessary, subculture of an NP clone was superinfected with a helper virus to rescue the sarcoma virus, and the rescued sarcoma virus-helper virus pseudotype complex was used for subcloning and further isolation of transformed NP clones.

Preparation of sarcoma virus-infected cell clones from CEF preinfected with RAV-60 was essentially similar to the isolation of the NP clones described above, except that CEF derived from an ev^- C/O embryo were used. The ev^- cells were used to reduce the complexity of subsequent provirus analyses. The ev^- CEF were infected with RAV-60 and transferred three times at 3-day intervals. The complete infection of cells with RAV-60 was checked by resistance to superinfection by RSV(chf) (20). These RAV-60-infected cells were then used for isolation of sarcoma virus-transformed colonies.

The NP clones of RSV(−) were prepared by direct fusion of RSV(−) virions to CEF by using UV-inactivated Sendai virus (19) and growing of the virus-fused cells in semisolid

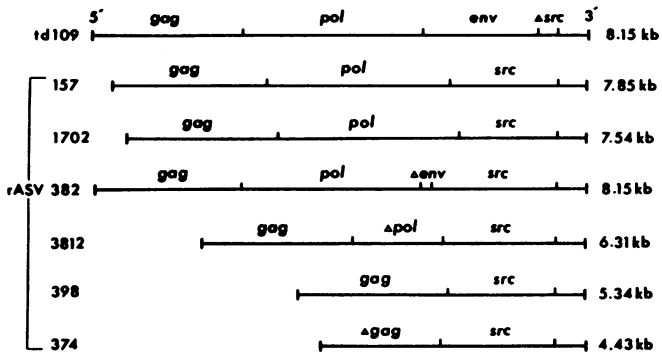

FIG. 2. Genomic structure of td109 and td109-derived rASVs (52). The RNA genomes of individual viruses are represented by the horizontal lines, and the size of each genome is shown at the right-hand side. The boundaries of the 5' *src* in td109-derived rASVs are heterogeneous (52). The remaining *env* in rASV382 represents the 5' *env* sequences, and the remaining *pol* in rASV3812 represents the 5' half of the *pol* gene. A portion of the 3' *gag* (P12 and P15 regions) is deleted in the rASV374 genome.

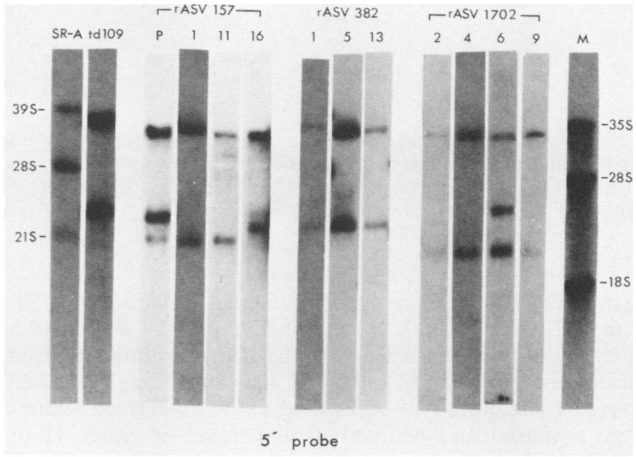

FIG. 3. Viral RNA patterns in *env*⁻ td109-derived rASV-infected cells. Five to ten micrograms of poly(A)-containing RNAs from either producer (P) or NP clones of rASV-infected cells was analyzed by RNA blotting and hybridization with ^{32}P-labeled viral DNA probes. The numbers represent individual NP clones. The 5' leader probe was used for the detection of viral RNAs. Analysis of RNAs from SR-A- or td109-infected cells were also included. ^{32}P-labeled 35S RAV-2 viral RNA, and 28S and 18S chicken rRNAs were used as molecular weight markers and are shown in lane M.

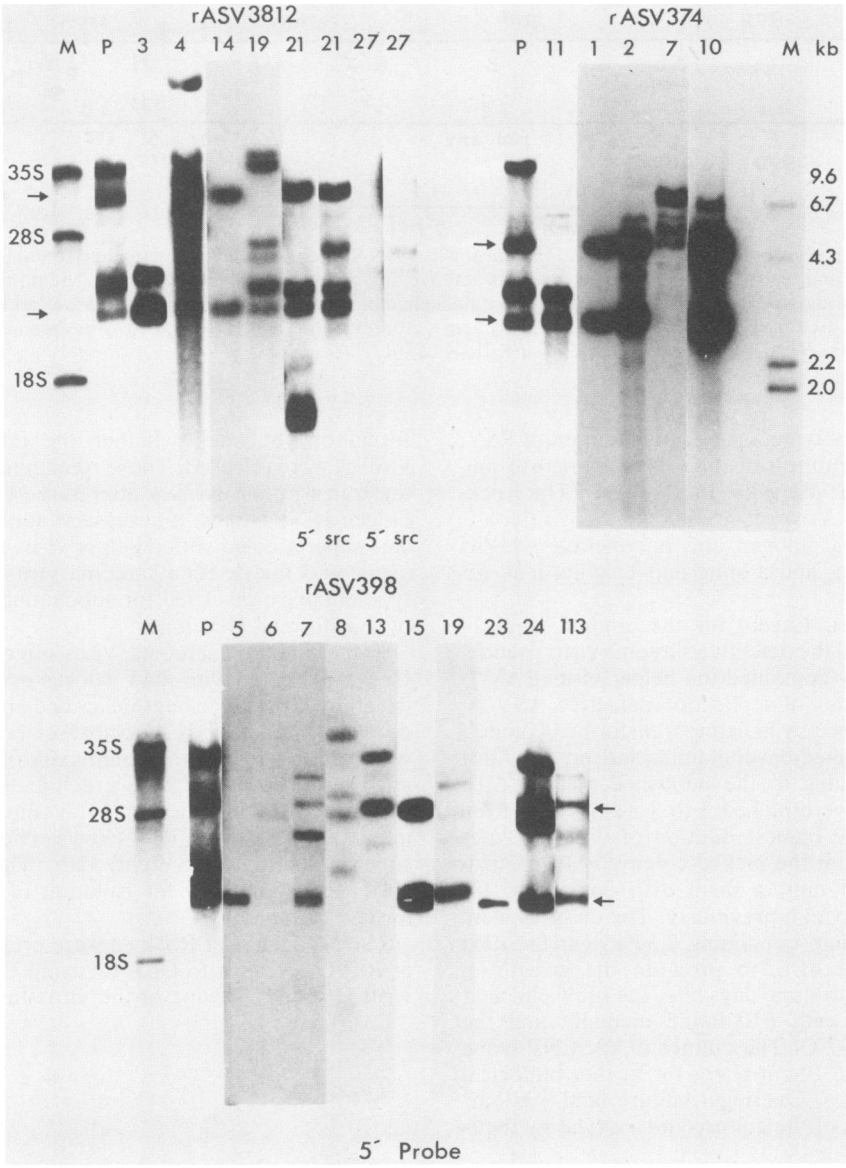

FIG. 4. Viral RNA patterns in *env*⁻ *pol*⁻ td109-derived rASV-infected cells. The experimental conditions and the designation of the figure are the same as described in the legend to Fig. 3. The 5′ probe was used for the hybridization of all clones. Hybridization with both 5′ and *src* probes is shown for clones 21 and 27 of rASV3812.[32]P-labeled lambda *Hin*dIII DNA fragments or RAV-2 and rRNAs were used as markers (lanes M). Arrows indicate the positions of expected genomic RNAs and *src* mRNAs of the sarcoma viruses.

agar medium at 41°C as described above. Infection of CEF with ts21, ts45, and ts337 was initiated at 37°C. Within 15 h of infection, cells were dispersed by trypsinization and used for colony formation in semisolid agar at 41°C as described above. Subcultures of individual ts virus-derived clones were prepared and maintained in parallel at either 41 or 37°C.

Preparation of DNA probes. Figure 1 depicts the origins of DNA probes used in this study. They were isolated from the following plasmid DNAs: pFC3 (obtained from F. Cross [52]), which contains the 5′ *Eco*RI fragment of SR-A (New York) DNA; PTT107 (50), which contains the 3′ *Eco*RI fragment of SR-A (New York) DNA; pSRA2 (8), which contains the entire SR-A (San Francisco) genome; lambda-td108 (54), which contains the entire genome of td108, a td virus derived from SR-A (New York); and pLTR-L6 (obtained from T. Takeya [52]), which contains the *Pvu*II to *Eco*RI DNA fragment of SR-B U3 region. In the initial experiments of this study, the strong-stop cDNA (22) prepared from RAV-2 or SR-A RNA (23) was used as the 5′ probe to detect the spliced subgenomic mRNAs. In the later experiments, the most 5′ DNA fragment shown in Fig. 1 was used. This DNA probe spans from the *Eco*RI site within the U3 region of the left-hand long terminal repeat (LTR) to the *Bam*HI site in the 5′ *gag* region of SR-A DNA with a length of ca. 500 nucleotides (8). Under our conditions of RNA analyses, i.e., the amount of RNA used, conditions for hybridization, and film exposure, this probe gave specificity similar to that of strong-stop cDNA probe.

DNA and RNA blotting and hybridization. Analyses of the

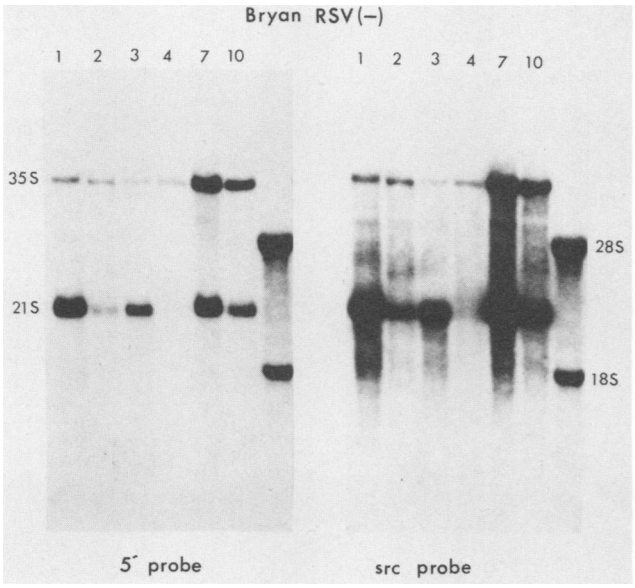

FIG. 5. Viral RNA patterns in RSV(−)-infected cells. RNAs prepared from individual NP clones of RSV(−)-infected CEF were analyzed by the procedure described in the legend to Fig. 3. The left panels show the patterns of hybridization with the 5′ probe, and the right panels show the patterns with the *src* probe.

genomic DNA of virus-infected cells with restriction enzymes were according to the method of Southern (46). The detailed conditions for hybridization and washing of DNA filters have been described (45). For analysis of intracellular viral RNAs, total polyadenylate [poly(A)]-containing RNAs were prepared from two to six 10-cm dishes of infected cells (23, 53). RNA from each sample (5 to 10 μg) was fractionated in 1% agarose gel and transferred to nitrocellulose paper by the method of Thomas (51). The RNA filters were hybridized with various probes according to the previously described conditions (55). To detect viral RNAs in the virions produced by the sarcoma virus-infected NP cells, 30 ml of medium was collected from a given NP cell culture. After cell debris was removed, the virus was pelleted for RNA extraction (53), and poly(A)-containing RNAs were isolated from that crude viral RNA preparation and then subjected to analysis as described above for intracellular viral RNAs.

RNase H digestion of the RNA:DNA hybrids. A total of 5 to 10 μg of total poly(A)-containing RNAs from virus-infected cells was hybridized with 100 ng of a given specific DNA fragment (see Fig. 1) in a 10-μl solution containing 25 mM sodium phosphate (pH 6.5), 0.6 M NaCl, 5 mM EDTA, 0.04% sodium dodecyl sulfate, 70% recrystalized formamide, and 0.5 mg of yeast RNA per ml. Hybridization was performed at 50°C for 15 h. The mixture was ejected into 100 μl of appropriate buffer afterwards, and the nucleic acids were precipitated by ethanol twice to remove formamide and salts. The RNA and DNA pellets were dissolved in water and divided into two portions; after the salt components were adjusted to the condition suitable for RNase H digestion according to the directions of the supplier of the enzyme, 1 unit of *E. coli* RNase H (Bethesda Research Laboratories) was added to one portion of the RNA:DNA hybrids. Both portions were incubated at 37°C for 20 min. They were then extracted with a phenol and chloroform mixture twice and precipitated by the addition of ethanol. The resulting RNA products were analyzed by gel electrophoresis, RNA blotting, and hybridization as described above.

RESULTS

RNA patterns in various sarcoma virus-infected CEF. Figure 2 depicts the genomic structure of td109-derived rASVs used in this study (52). All of the td109-derived rASVs contained *env* deletions. Three isolates contained more extensive deletions: rASV3812 deleted the 3′ half of *pol* in addition to *env*, rASV398 deleted all of *pol* and *env*, and rASV374 deleted 3′ *gag* in addition to *pol* and *env*. It has been shown recently that the *src* seletion in td109 extends beyond the splicing acceptor site (52), located at 76 nucleotides upstream from the AUG codon for $pp60^{src}$, for the synthesis of 21S *src* mRNA (49, 50). Initially, I was interested to know the origin and location of the new splicing acceptor site for the synthesis of the *src* mRNAs of td109-derived rASVs. As an approach to this question, I analyzed the viral RNAs present in rASV-infected cells.

Results (Fig. 3) show that env^- rASV-infected NP or producer cells displayed a normal pattern of genomic RNAs and spliced *src* mRNAs. The slightly larger *src* mRNA seen in rASV382-infected cells and the slightly smaller one in rASV1702-infected cells are expected because their genomic RNAs contain extra 5′ *src* sequences and a 5′ *src* deletion, respectively (52). An unexpected 3.5-kilobase (kb) RNA species was observed in rASV1702 clone 6. This RNA most likely resulted from downstream promotion of the cellular sequence next to the integration site (see below). Similarly, the producer cells infected with the three env^- pol^- rASVs also produced expected viral RNAs, including genomic RNAs and spliced *src* and *env* mRNAs of the sarcoma and helper viruses (Fig. 4, lanes P). This is true for cells directly infected with the mixture of helper and sarcoma viruses or cells derived from a single colony doubly infected with both viruses.

These results show that a new splicing acceptor site presumably derived from c-*src* sequences is used for the processing of *src* mRNA in td109-derived rASVs. The relative location of this site from the beginning of *src* coding sequence appears to be equivalent to that of RSV genome, since the size of the *src* mRNAs of td109-derived rASVs is similar to that of SR-A (Fig. 3 and 4). This is consistent with the result of S1 mapping of the splicing acceptor site for 26S c-*src* mRNA (48). For rASV157 and rASV1702, however, data presented here cannot show whether the newly obtained c-*src* splicing acceptor site or the original *env* mRNA splicing acceptor site is used for the synthesis of *src* mRNA, since mRNAs resulting from either site would not be resolved in the gel under our conditions. The larger *src* mRNA seen in rASV382 implies that either the *env* splicing acceptor site or a site upstream from the one located previously on c-*src* mRNA is used.

In contrast to the normal RNA patterns seen in the env^- rASV-infected cells, the NP clones of the three env^- pol^- rASVs gave unexpected patterns of viral RNAs (Fig. 4). RNAs larger than the genomic size and in between the genomic RNA and normal 21S *src* mRNA were observed in most NP clones of these rASVs. Some clones contained no normal-sized genomic and subgenomic *src* RNAs. The overall pattern and the relative abundance of individual species of mRNA varied from one clone to another. Judging from the intensity of RNA bands in Northern blots, the amount of viral RNAs per microgram of total poly(A)-containing RNAs

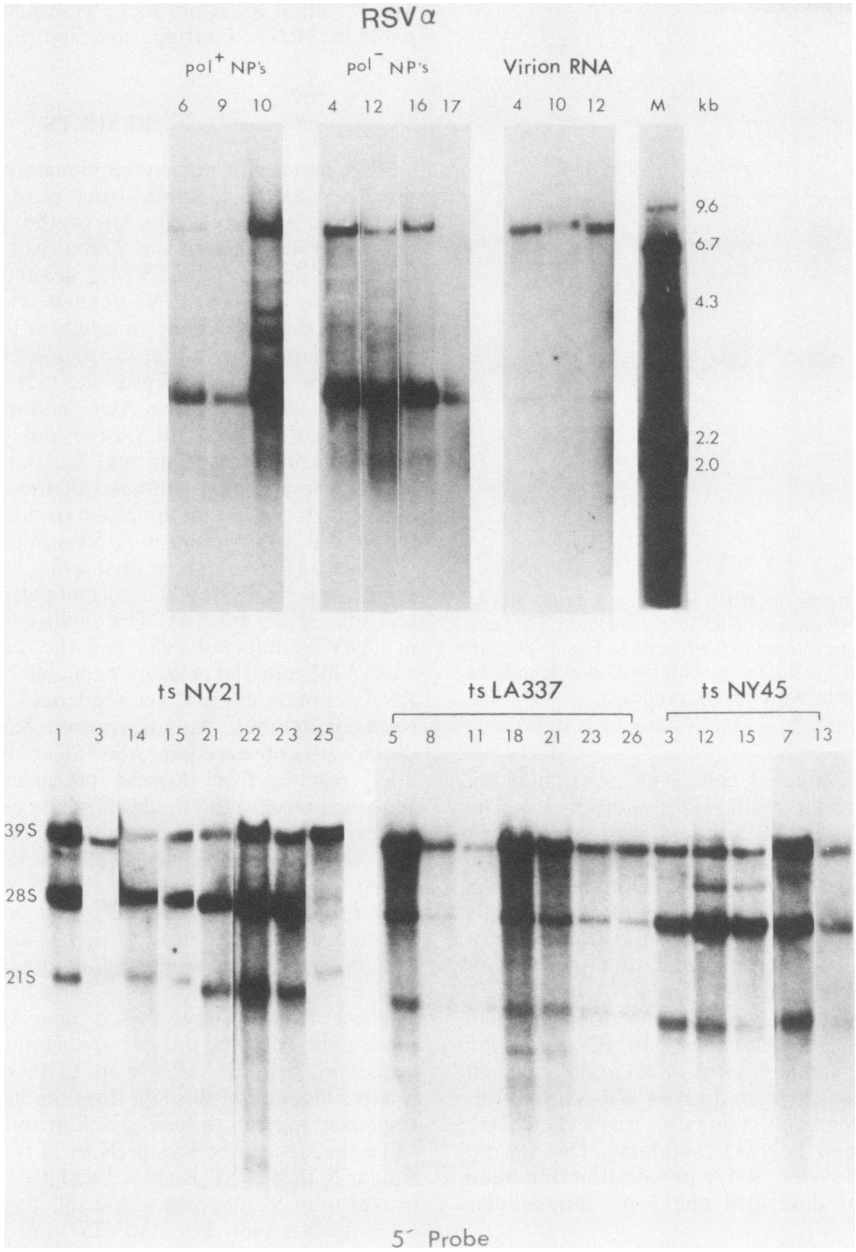

FIG. 6. Viral RNA patterns in RSVα- and ts *pol* RSV-infected cells. For RSVα, NP clones were isolated from the RSVα (RAV-1) pseudotype, and both *pol*$^+$ and *pol*$^-$ clones were obtained. For the analysis of virion RNA, 30 to 50 ml of medium supernatant from NP clones was harvested. After cell debris was removed, viral particles were pelleted for the extraction and selection of poly(A)-containing RNAs. For ts *pol* RSV-derived clones, subcultures of each clone were kept at either the permissive or nonpermissive temperature. The same RNA patterns were observed for either temperature.

from *env*$^-$ *pol*$^-$ rASV-infected cells, however, was comparable to those from *env*$^-$ rASV or replication-defective RSV-infected cells (Fig. 3, 4, 5, and 6). This implied that the efficiency of transcription in those defective rASVs was not impaired by the deletions. With the exception of an abundant 1.6-kb RNA detected in rASV3812 clone 21, all those unusual-sized subgenomic RNAs contained *src* sequence (also see below) and were spliced because they hybridized to the 5′ probe. Similar to the unexpected 3.5-kb RNA seen in rASV1702 clone 6 described above (Fig. 3), this 1.6-kb RNA was most likely generated by downstream promotion of the cellular sequences, since it hybridized only to the 5′ probe (see below). Most of the NP clones produced noninfectious viral particles containing only genomic and supergenomic RNAs (52; data not shown).

To see whether these phenomena with the three *env*$^-$ *pol*$^-$ td109-derived rASVs occur with nondefective RSV and other defective RSV of independent origins, single colony-derived cultures of rASV1441 and SR-A and NP clones of BH RSV(−) and SR NY8 were similarly prepared and analyzed. Results of such analyses indicated that essentially only the normal-sized viral RNAs were produced in the

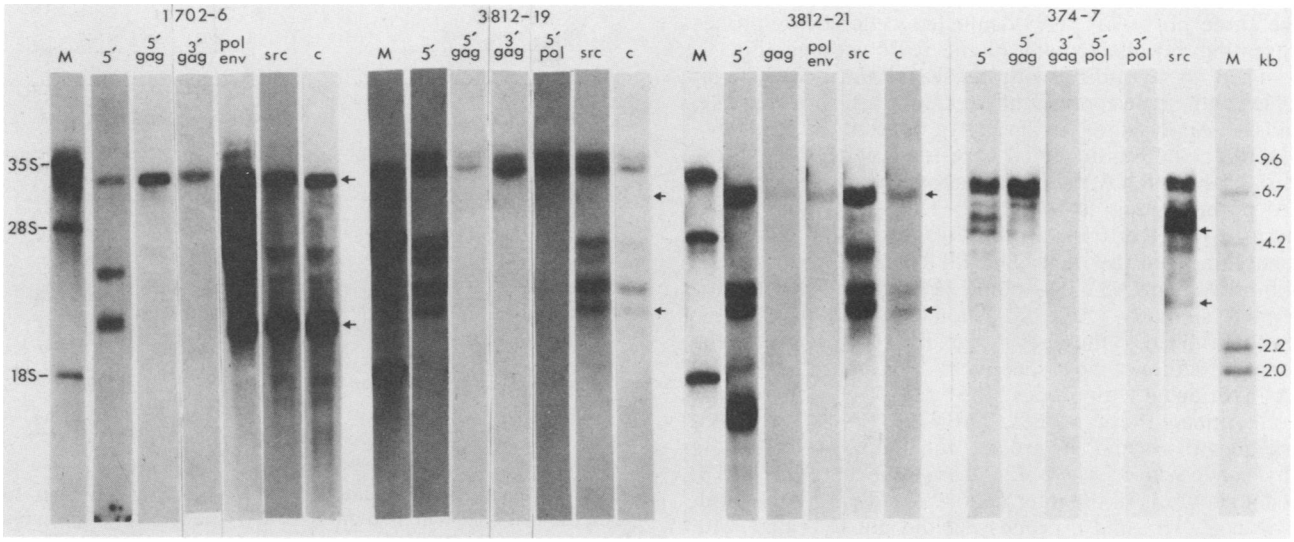

FIG. 7. Sequence content in mRNAs of various rASV-infected NP cells. The RNAs of certain representative NP clones of *env* and *env pol*$^-$ rASV-infected cells were analyzed by sequential hybridization of the same RNA blot with various probes. Arrows point to the positions of normal-sized genomic RNAs and *src* mRNA for each rASV.

infected cells (result for RSV(−) is shown in Fig. 5; other data not shown). Results for RSV(−) and SR NY8 agree with those of *env*$^-$ td109-derived rASVs. It is concluded that deletion of *env* has no effect on the RNA expression.

Since the aberration of viral RNA expression correlated with the deletion in *pol*, I then checked whether lack of *pol* function was responsible for the abnormality. A nonconditional and three conditional *pol* mutants were analyzed similarly. Not surprisingly, some of the NP clones derived from the RSVα (RAV-1) pseudotype complex were *pol*$^+$ (Fig. 6). This phenomenon has been described before (16, 44). Both *pol*$^+$ and *pol*$^-$ NP clones exhibited only the normal-sized genomic RNA and *src* mRNA and produced virions containing essentially only the genomic RNA. Similarly individual clones of ts *pol* mutant-infected CEF displayed the expected viral RNA pattern at either the permissive or nonpermissive temperature. Viral RNAs running between 28S and 39S RNA markers were detected in clones 7, 12, and 15 of tsNY45. The origin of these RNAs is not clear, but it may derive from the deletion variants present in the tsNY45 virus stock. These results demonstrate that lack of *pol* function is not responsible for the abnormality of RNA patterns in the three *pol*$^-$ *env*$^-$ rASVs.

Sequence content in the mRNAs of *env*$^-$ *pol*$^-$ rASV. To

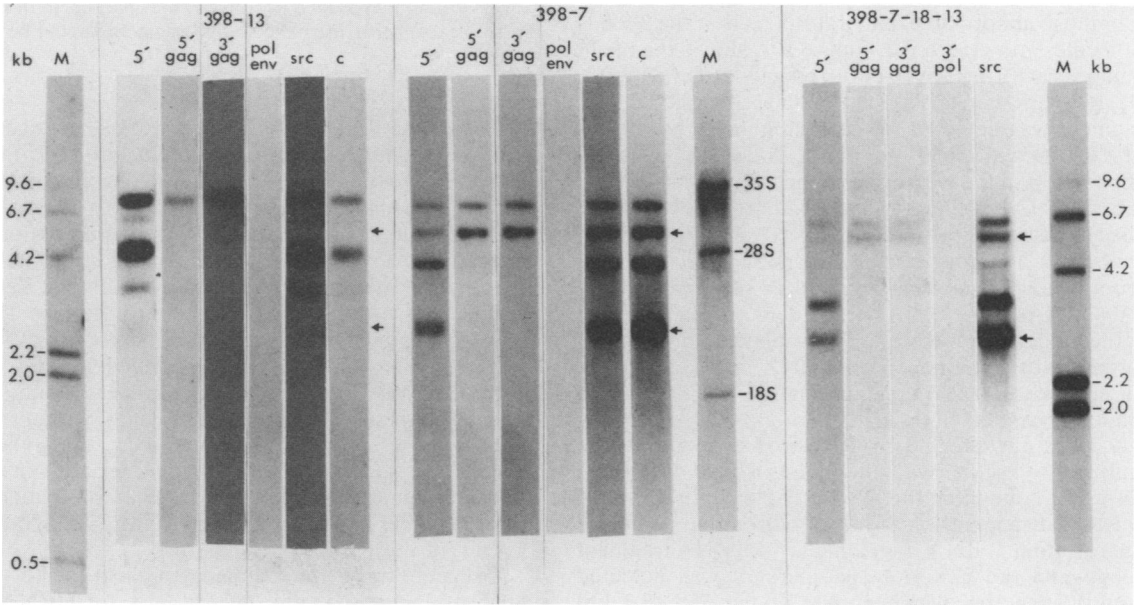

FIG. 8. Sequence content in mRNAs of rASV398-infected NP cells. Conditions were similar to those described in the legend to Fig. 7. Arrows point to the positions of normal-sized genomic RNA and *src* mRNA of rASV398.

analyze the nature and origin of the unusual mRNAs present in the three *pol*$^-$ *env*$^-$ rASV-infected cells, DNA probes representing various regions of the RSV genome (Fig. 1) were used to hybridize with those mRNAs. Results of analyses with some representative clones are shown in Fig. 7 and 8. Analysis of viral RNAs present in the *env*$^-$ rASV1702 clone 6 is included here to show that the unexpected 3.5-kb mRNA mentioned above hybridized only to the 5′ probe among all viral probes tested (Fig. 7), most likely as a result of transcription of the cellular sequences downstream from the right-hand LTR of the provirus. The 1.6-kb mRNA in rASV3812 clone 21 (Fig. 7) was probably generated similarly. All the genomic and supergenomic RNAs hybridized to the viral probes in accordance with the genomic structure of the respective rASV (Fig. 2). rASV3812 RNAs hybridized with probes 5′, 5′ *gag*, 3′ *gag*, 5′ *pol*, *src*, and *c*. Among these probes, rASV398 RNAs could not hybridize with *pol* and *env* probes, and rASV374 RNA could not hybridize with 3′ *gag*, *pol*, and *env* probes. (Fig. 7 and 8; data not shown.) All the intermediate-sized mRNAs hybridized with 5′, *src*, and *c* probes but did not hybridize with probes derived from regions between the 5′ leader and *src* sequences. (The 4-kb *src* containing RNA in rASV3812-21 clone is apparently the c-*src* mRNA.) These results indicate that the unexpected intermediate-sized mRNA are not generated by splicing to alternative acceptor sites upstream from *src*. Besides, alternative splicing certainly cannot account for the generation of supergenomic RNAs.

Location of the extra sequences on the unusual-sized mRNAs. The above-described results also imply that the extra sequences in those unexpected mRNAs were probably derived from cellular sequences, perhaps as a result of upstream initiation of transcription from cellular into viral sequences or downstream polyadenylation of the primary RNA transcript. The former would predict the extra sequences to be located at the 5′ end of the mRNAs, and the latter would predict the location to be at the 3′ end of the mRNAs. To resolve these alternatives, experiments schematically shown in Fig. 9 were performed. Generation of a uniform 5′ RNA fragment and heterogeneous 3′ RNA fragments upon RNase H digestion would indicate that the location of extra sequences in those abnormal-sized viral RNAs is at the 3′ ends of the molecules and vice versa. Figure 10A shows the result of such analyses with mRNAs from an NP clone of rASV3812, clone 11, and various rASV398 NP clones. A uniform 2-kb RNA fragment was detected for each clone after hybridization of the RNAs with the 3′ *gag* DNA, followed by RNase H digestion and probing with either 5′ or 5′ *gag* DNA probe. This 2-kb 5′ RNA fragment was indistinguishable in size from those generated by the control RNAs from SR-A-infected cells and a producer clone of rASV3812, clone 9, which contained the normal-sized rASV3812 and helper virus td108 RNAs. The RNAs treated in parallel, except without the addition of RNase H, displayed the original RNA pattern with some nonspecific RNA degradation, but revealed no 2-kb RNA fragment (lanes −). The spliced subgenomic RNAs of both producer and NP clones of rASV3812 were not affected by RNase H digestion, since they could not hybridize with the 3′ *gag* DNA. When the same RNA blot containing the RNase H-cleaved rASV3812 mRNAs was subsequently hybridized with an *src* probe to detect the resulting 3′ RNA fragments, a 4-kb RNA fragment running between the 22S and 28S markers was detected (concurrently with the disappearance of the 32S [6.3 kb] rASV3812 genomic RNA) in the control rASV3812 clone 9 RNA preparation; the 21S (3-kb) *src* mRNA remained unaffected (clone 9, lane +). Without RNase H digestion, both the 32S and 21S RNAs were intact (clone 9, lane −). As expected, neither species of the helper viral RNAs, which lacked the *src* sequence, was revealed by the *src* probe. By contrast, clone 11 revealed upon hybridization with *src* probe three to four RNA species ranging from 4 to 5.5 kb concurrent with the disappearance of genomic RNA and two species of supergenomic RNAs after RNase H digestion (clone 11, lane +). The size of the fastest migrating 3′ RNA fragment from clone 11 corresponded to that of clone 9 control RNAs. The genomic and supergenomic RNAs remained detectable in the control lanes without RNase H, although the amounts were reduced, apparently due to nonspecific degradation during the process of treatment. These results demonstrate that the extra sequences in the supergenomic RNAs are located at the 3′ end, but not at the 5′ end, of the RNA molecules.

To locate the extra sequences present in the subgenomic mRNAs larger than the normal 21S *src* mRNA, the total poly(A)-containing RNAs from two rASV3812-derived NP clones (clones 7 and 11) and a producer clone (clone 9) were

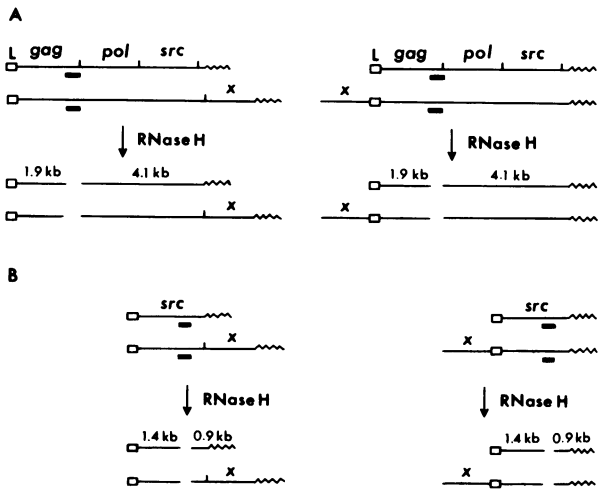

FIG. 9. Schematic illustration of the RNase H experiments to locate the extra sequences in mRNAs. (A) The rASV3812 genomic and supergenomic RNAs are represented by the horizontal lines. The open boxes and wavy lines depict the 5′ leader and 3′ poly(A) tails, respectively. For the left-hand side of the panel it is assumed that the extra sequence (designated *x*) in the supergenomic RNA is located at the 3′ end, presumably by read-through transcription and altered cleavage site; the right-hand side of the panel predicts the 5′ location of *x* sequence, presumably by upstream initiation of transcription. When the RNAs are hybridized to a 3′ *gag* 400-base-pair DNA fragment (represented by thickened bars, also see Fig. 1) and subsequently digested with RNase H, the normal genomic RNA should yield a 5′ 1.9-kb and a 3′ 4.1-kb RNA fragment detectable by 5′ and 3′ viral probes, respectively. Generation of expected 5′ RNA fragments and unusual-sized 3′ RNA fragments longer by *x* sequence would indicate its location to be at the 3′ end and vice versa. (B) When the spliced subgenomic *src* RNAs are hybridized to a 3′ *src* 366-base-pair DNA and digested with RNase H similarly, the normal *src* mRNA should yield a 5′ 1.4-kb fragment and a 3′ 0.9-kb fragment detectable by 5′ probe and 3′ *src* probe, respectively. Again, the sizes of 5′ and 3′ RNA fragments generated should allow one to assess the location of the extra sequence. Resulting products from genomic and supergenomic RNAs after hybridization with the 3′ *src* DNA and RNase H treatment are not depicted here, but the digestion should produce RNA fragments parallel to those described in (A), except that the expected 5′ fragment should be ca. 5 kb.

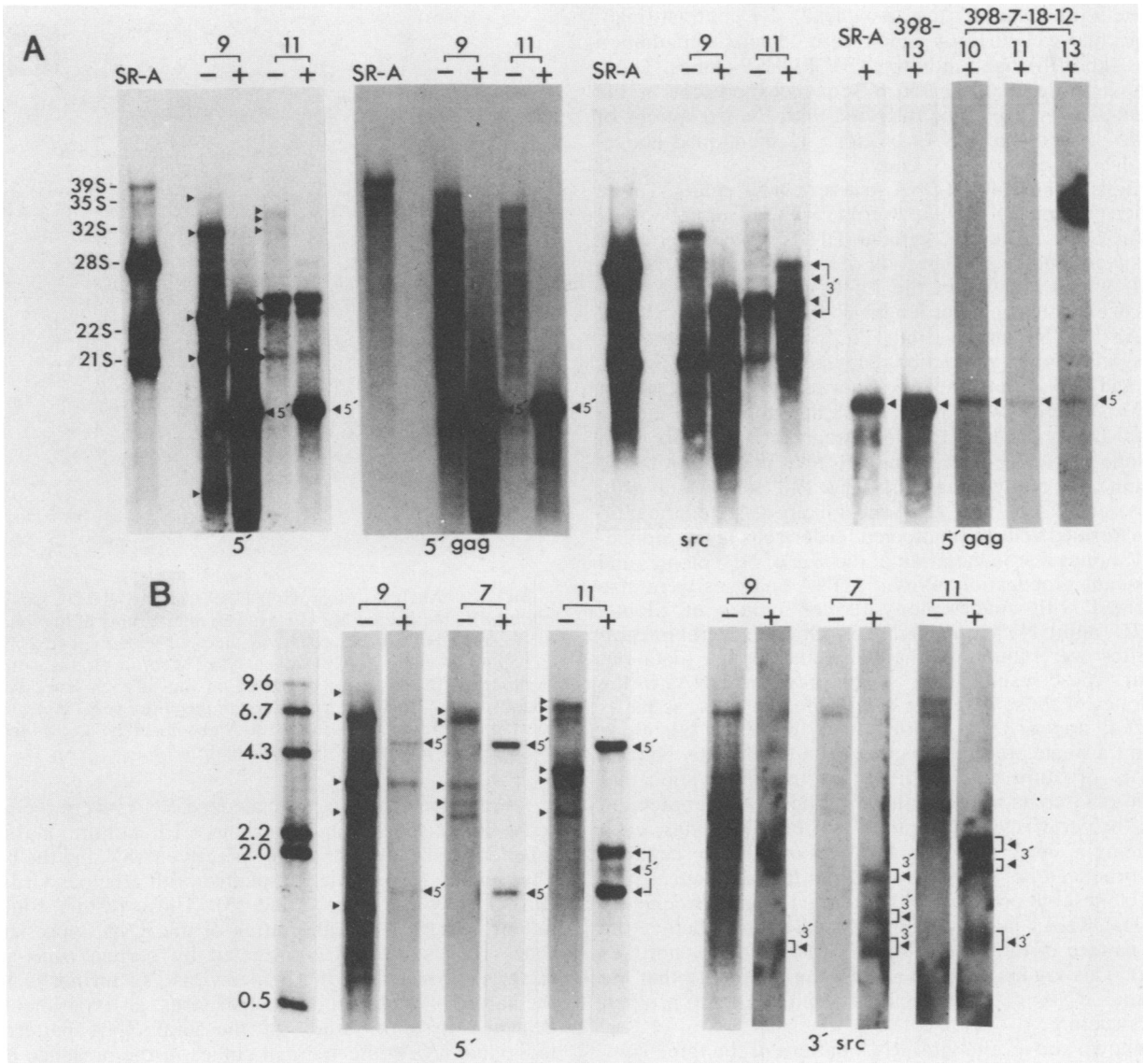

FIG. 10. Mapping of the extra sequences in viral RNAs by RNase H digestion. Details of the experiments are described in the text. A producer clone, clone 9, and two NP clones, clones 7 and 11, of rASV3812, as well as four NP clones of rASV398 (398-13 and three 398-7-derived subclones, subclones 10, 11, and 13) were analyzed. Clone 9 contained normal-sized rASV3812 and helper virus td108 RNAs, including genomic and spliced subgenomic RNAs of both viruses. The two rASV3812 NP clones, clones 7 and 11, contained five and six species of viral RNA, respectively, in the infected cells. Mixtures of SR-A and td SR-A RNAs shown in the first three panels from the left in (A) served only as molecular weight markers and were not included in the RNase H experiment. The + and − lanes represent pairs of duplicate samples treated in parallel throughout the experiment, except for the addition or omission of RNase H at the digestion step. The panels in (A) show the results of the experiment with 3′ *gag* DNA, and the panels in (B) show the results of using 3′ *src* DNA (See Fig. 1 and 9 for the DNA locations). The rightward-pointing arrows indicate the positions of viral RNA species in each clone before treatment. The 5′ and 3′ RNA fragments generated by RNase H digestion are indicated by leftward-pointing arrows. The probe used is indicated at the bottom of each panel. The first three panels from the left in (A) show RNA patterns revealed by sequential hybridization of the same RNA blot with 5′, 5′ *gag*, and *src* probes. Similarly the panels in (B) show the result of sequential hybridization with 5′ and 3′ *src* probes.

hybridized with the 366-base-pair *Pst*I-*Bgl*I *src* fragment (Fig. 1) and analyzed as described above. The results showed that a 5-kb RNA species presumably derived from the rASV3812 genomic RNA and a 1.4-kb species presumably derived from the 21S *src* mRNA were detected by 5′ probe upon RNase H digestion of clone 9 control RNAs (Fig. 10B). The td108 helper viral RNAs were not affected by the DNA hybridization and RNase H digestion, although nonspecific degradation had apparently occurred during the treatment. Two RNA species of similar size were generated from viral RNAs of clones 7 and 11. However, a 2- and a 1.8-kb RNA species were also seen in clone 11. These two RNA species were apparently derived from the subgenomic RNAs, since supergenomic RNAs gave rise to only a uniform 5′ RNA fragment (Fig. 10A). It is possible that the 1.8-kb and 2.0-kb RNAs resulted from splicing of the leader sequence to the sites upstream from the normal 21S *src* mRNA splicing acceptor site. This has never been seen with other NP clones (see above). When a 3′ *src* probe was used for the hybridization, a ca. 1-kb diffuse RNA band was seen

in clone 9 (indicated by the arrowhead). By contrast, higher-molecular-weight RNA bands were detected, in addition to the 1-kb RNA band in both rASV3812 NP clones. These results indicate that the extra sequences present in the unusual-sized subgenomic mRNAs, with the exceptions of the two subgenomic RNAs of clone 11 mentioned above, were also present in the 3′ end.

Analysis of the proviral DNA structure in NP clones. To see whether the unusual RNA patterns resulted from abnormal proviral DNA structure, cellular DNAs from several NP clones were analyzed. Digestion of the DNAs with *Pvu*I or *Eco*RI, which cut within the LTR, generated DNA fragments of expected genomic length from rASV1702, rASV398, and rASV374 NP clones (Fig. 11). Analyses of the proviral DNAs with other restriction enzymes, including *Hin*cII, *Bgl*I, and *Bgl*II, detected no abnormality either (data not shown). Digestion with *Sac*I, which had no cuts within the proviral DNA, generated a DNA fragment specific to each NP clone of rASV, RSVα, and SR NY8 in addition to the common c-*src* related fragments (Fig. 12). Relative intensity of proviral DNA to c-*src* DNA most likely reflected the ratio of transformed cells to uninfected feeder cells in the individual NP clones due to variation of the size of NP colonies and subsequent propagation. Proviral DNA analyses were also performed with single-colony-derived clones of SR-A-, tsNY21-, and tsNY45-infected cells. One to several integration sites were found in the individual clones (data not shown). These results show that the proviral DNAs in the NP clones of those defective rASV-infected cells, as far as analyzed, appear to be normal and that each NP clone contains a single proviral integrated at a unique site. Normal provirus structure was confirmed by the observation that infectious sarcoma viruses can be rescued by superinfection with a helper virus to essentially all the NP clones, each containing a single provirus. Furthermore, the rescued viruses produced normal-sized RNAs in the subsequent producer clones, but produced either normal or more frequently abnormal RNAs in NP clones, regardless of whether the RNA pattern of the parental clone was normal or not (see below). This argues strongly against the possibility that the abnormal RNA patterns resulted from aberrant proviral DNA structure.

As shown above, the viral RNA pattern of the three *env*$^-$ *pol*$^-$ rASVs is specific to each NP clone, which is shown here to contain a single provirus at a unique site. Therefore, it can be concluded that the RNA pattern of those *env*$^-$ *pol*$^-$ rASVs is a function of the integration site. This is not so in the rest of the ASVs analyzed and described above, including RSV(−), SR NY8, and RSVα. However, RSVα has been shown to contain no detectable *pol* deletion (31).

Effect of subcloning and helper virus infection on the RNA patterns of *env*$^-$ *pol*$^-$ rASVs. It could be argued that variation of the viral RNA patterns among NP clones might not be due to the effect of integration sites, but rather due to the presence of variant viruses in the stocks of the three *env*$^-$ *pol*$^-$ rASVs. To investigate this possibility, a given NP clone was superinfected with the helper virus RAV-1, and the rescued rASV (RAV-1) pseudotype was subjected to further biological cloning for isolation of NP clones and analysis of viral RNAs. The result with rASV398 is shown in Fig. 13. It can be seen that upon each of the three cycles of subcloning, the viral RNAs of each progeny NP clone varied from one to another and was distinct from the parental clone. A similar result was also obtained with rASV3812 (data not shown). These results confirmed the conclusion of the effect of the integration site on the viral RNA pattern.

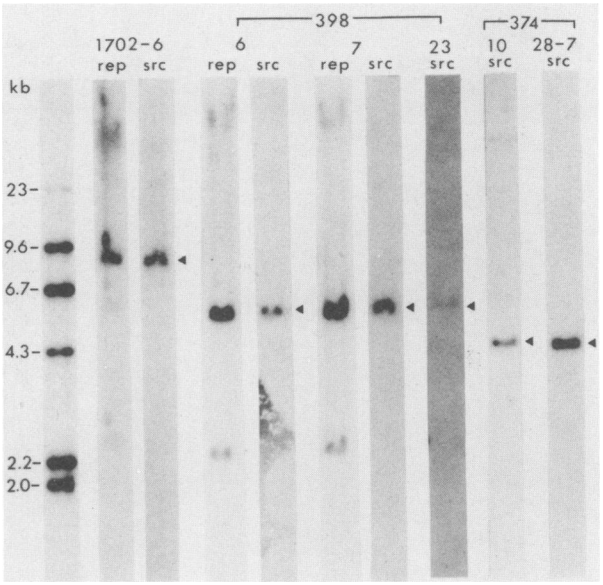

FIG. 11. Analyses of proviral DNAs in rASV1702-, rASV398-, and rASV374-infected NP clones. Ten micrograms of high-molecular-weight DNAs of NP cells was digested with *Pvu*I (except that *Eco*RI was used for 374-10) and analyzed according to the method of Southern with the probe indicated on top of each lane. The rep probe resulted from nick translation of the entire pSR2 insert (8) and therefore represents the entire SR-A genome. The arrows indicate the expected proviral DNA fragments.

As mentioned above, normal-sized RNAs were the prominent RNA species in either the CEF culture massively infected with a mixture of the defective rASV and the helper virus or the NP cells superinfected with a helper virus and further passaged (Fig. 4 and 13). These results could be taken to suggest that aberration of the RNA expression in those rASVs could be corrected by certain *trans*-acting factor(s) provided by the helper virus. To further examine the nature of the effect of a helper virus, an experiment was designed to allow study of the viral RNA patterns of individual rASV-infected cell clones in the presence of the helper viral function, but without reinfection of the rASV (helper virus) pseudotype. This was done by cloning the rASVs on C/O CEF preinfected with subgroup E virus, RAV-60, and subsequent plating of the individual transformed colonies on C/E CEF (see above). Results of such experiments showed that the RNA patterns remained abnormal in the presence of helper viral functions when there was no virus spreading (Fig. 14). Therefore the normal RNA patterns seen in the helper virus-superinfected and passaged NP clones appeared to be due to infection and spreading of the rescued rASV on the feeder CEF and the original NP cells. Virus spreading inevitably would randomize the original integration site in the NP clone. The specific RNA species resulting from individual integration sites would add up only to a smearing background, on top of which would be the normal-sized RNAs which were common among different integration sites. Indeed, this was seen in the helper virus-superinfected NP clones (Fig. 13) and in the cells massively infected by rASV and helper virus (Fig. 4; data not shown). It is concluded that the aberration of RNA expression in those *env*$^-$ *pol*$^-$ rASVs is due to a *cis* effect and cannot be complemented directly by the helper viral functions.

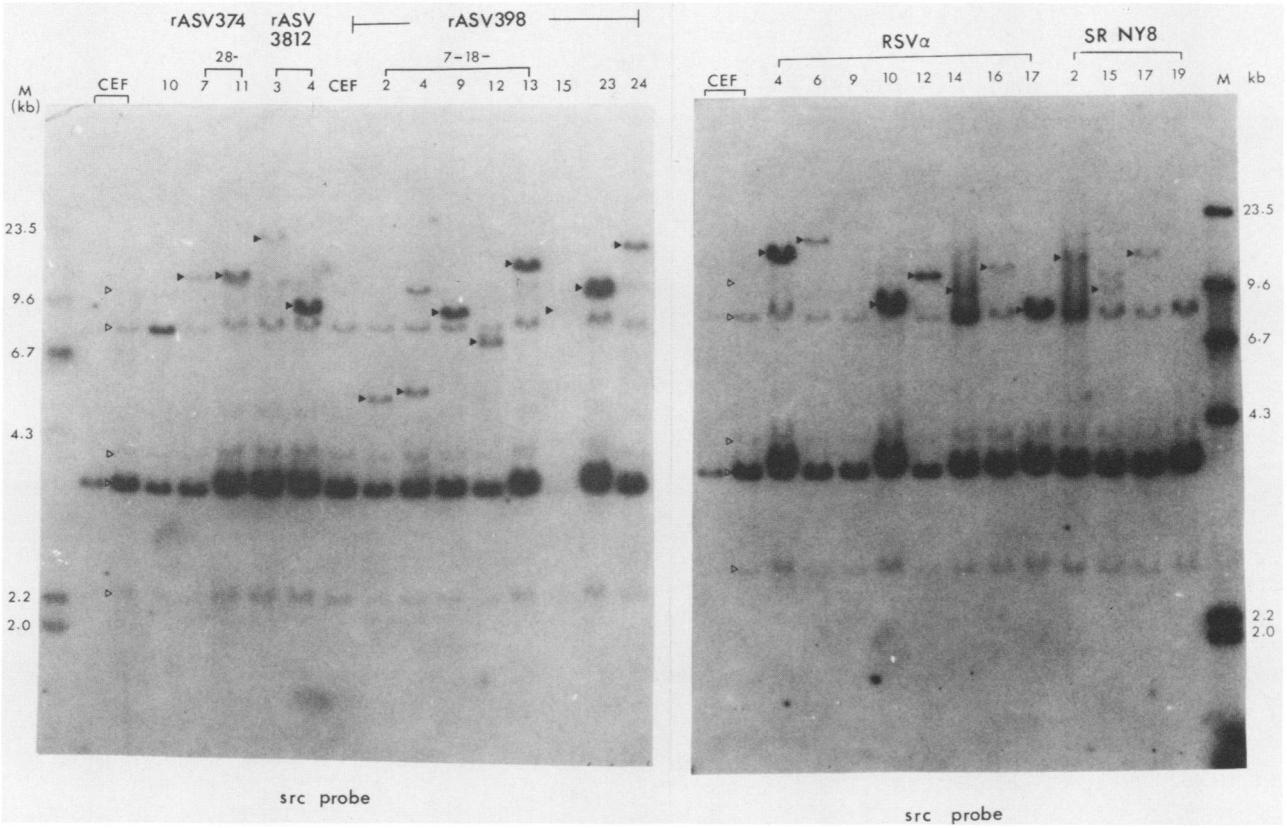

FIG. 12. Analyses of proviral DNAs in various rASV- and defective RSV-infected NP cells. Conditions were similar to those described in the legend to Fig. 11, except that restriction enzyme *Sac*I was used for the digestion. The open arrowheads indicate the normal chicken cellular *src*-related DNA fragments; the solid arrowheads indicate the provirus-containing DNA fragments in the individual NP clones.

DISCUSSION

New *src* mRNA splice acceptor site in rASVs. The results presented above indicate that a new splicing acceptor site for *src* mRNA, along with the deleted *src* sequences, have been reinstated into the td109 genome after recombination with c-*src* sequences. In most of the td109-derived rASVs analyzed here it is not clear whether the normal c-*src* 26S mRNA splicing acceptor site or a new site is used for the synthesis of *src* mRNA. In the case of *env*$^-$ rASVs, the *env* splicing acceptor site may be functional even if a new site is not regenerated for the *src* mRNA. This is not the case for the three *env*$^-$ *pol*$^-$ rASVs, for which a new *src* mRNA splicing acceptor site must have been reinstituted, since the *env* and at least the 3′ half of *pol* containing the *env* mRNA splicing acceptor site were deleted in their genomes. Most likely a site other than the regular c-*src* mRNA splicing acceptor site is used in rASV382, since its *src* mRNA is ca. 300 nucleotides larger than the normal 21S *src* mRNA. Preliminary sequence analysis of rASV3812 also indicated that the sequences containing the 26S c-*src* mRNA splicing acceptor site was not incorporated into the rASV3812 genome (unpublished data).

Deletion in *pol* correlates with aberrant RNA expression. The appearance of the supergenomic RNAs and unexpected subgenomic *src* mRNAs in the three replication-defective rASV-infected cells appears to correlate with the deletion of the 3′ portion of *pol*. This is inferred since neither the *env*$^-$ rASVs derived from the same parental virus td109 nor the *env*$^-$ RSV, RSV(−), and SR NY8 are abnormal in the mRNA expression. Some of the td109-derived rASVs contain additional sequences upstream from the coding region of *src*, and these sequences are presumably derived from the c-*src* (52). However, the presence of these sequences has no correlation with the aberrant RNA patterns, since rASVs containing various lengths of those upstream sequences displayed either normal (rASV382) or abnormal (rASV3812 and rASV374) RNA patterns; furthermore, rASV398 does not contain those sequences and displayed an abnormal RNA pattern. Moreover, our preliminary experiment with one of the *env*$^-$ *pol*$^-$ rASVs showed that the RNA expression was normal when the 3′ *pol* sequence was inserted back into the viral genome (unpublished data). The defectiveness in the RNA expression is not due to the lack of *pol* function and cannot be complemented in *trans* by helper virus functions. Unusual-sized viral RNAs were observed previously in mutaginized Prague RSV-infected NP quail cells (33, 34) and in acute leukemia virus OK10-infected chicken bone marrow cells (42). Most of the abnormal-sized RNAs seen in Prague RSV quail cells could be accounted for by the deletions present in the proviruses; however, some of those mRNAs were larger than the genomic length. The possibility of the presence of cellular sequences in those supergenomic RNAs was raised; however, the basis for the generation of those RNAs was not explored in those studies.

Origin of the abnormal-sized viral RNAs and hypothesis for 3′ end processing of ASV RNA. Both the supergenomic RNAs and the unusual-sized subgenomic *src* RNAs in the three *env*$^-$ *pol*$^-$ rASV-infected cells contain extra sequences at the 3′ ends of the viral RNAs. These extra sequences most

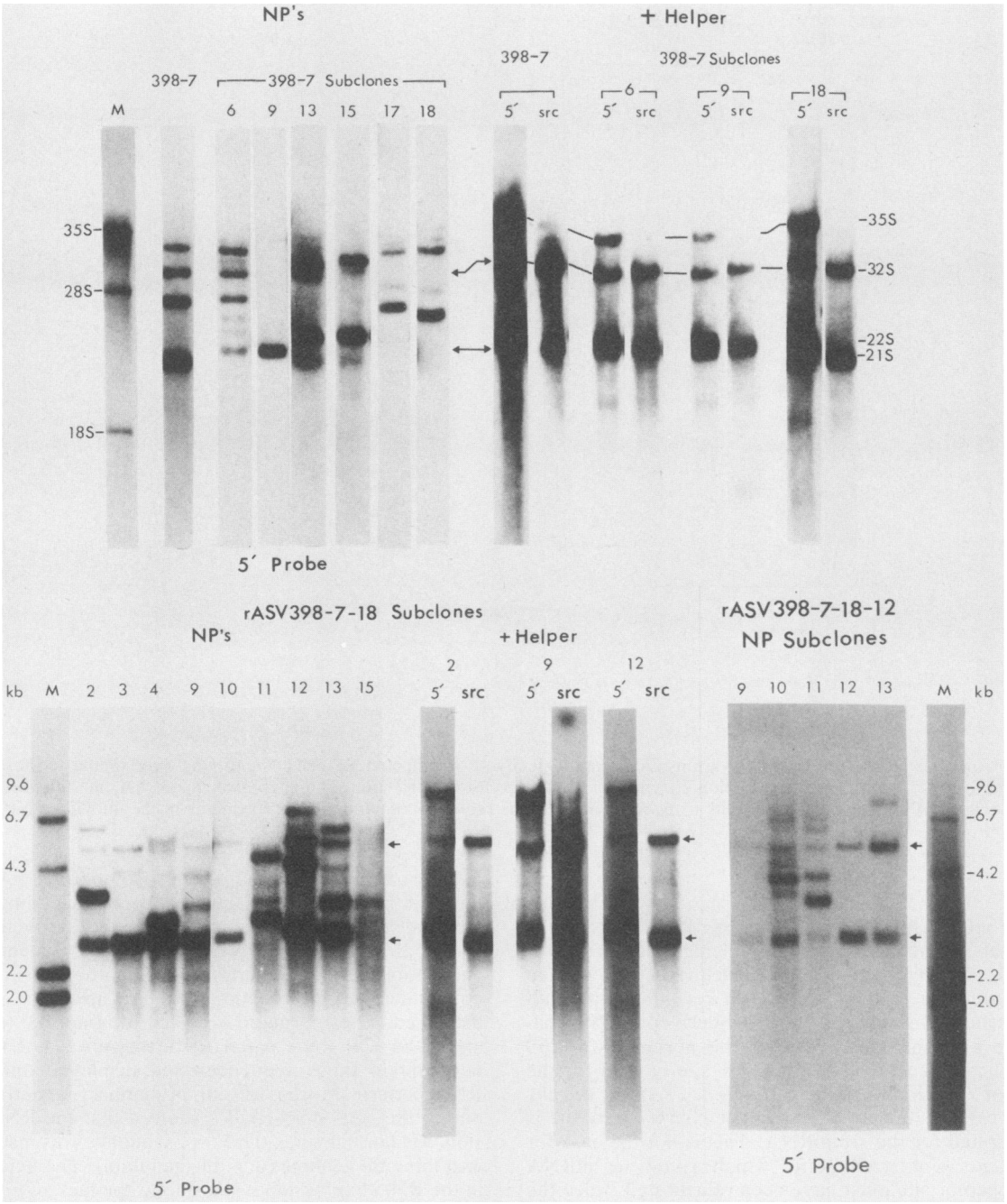

FIG. 13. Subcloning of the *env*⁻ *pol*⁻ rASVs. rASV398 NP clone 7 was rescued with RAV-1 and further cloned in three subsequent cycles. RNAs were isolated from individual NP clones of each cycle of subcloning for analysis. Helper virus RAV-1 was added to parallel cultures of certain NP clones to rescue the defective sarcoma virus for subsequent cloning. After four to five transfers of helper virus-superinfected cultures, RNAs were also isolated for analysis. For NP clones, RNA patterns detected with the 5′ probe are shown; for helper virus-superinfected cultures, patterns resulting from hybridization with either 5′ or *src* probes are shown.

likely were derived from the cellular sequences by read-through transcription of the proviral DNA. The extent of read-through sequences is a function of the chromosomal location of the provirus. This could then explain the variation of mRNA patterns among the NP clones. I propose that the aberration is due to cleavage and polyadenylation at multiple sites of the 3′ region of the primary viral RNA transcript in those defective sarcoma virus-infected cells. In general, transcription of viral and eucaryotic genes has been shown to pass beyond the polyadenylation site (9, 10, 25, 40). Cleavage of the primary RNA transcript, followed by polyadenylation, occurs specifically within 10 to 20 nucleotides downstream from the AAUAAA sequence universally present near the 3′ end of viral and eucaryotic mRNAs (2, 7, 39, 58). Unless the transcription of retroviral DNA represents an exception, it can be assumed that transcription of wild-type RSV provirus also continues beyond the polyadenylation site. Indeed, it was shown recently that certain

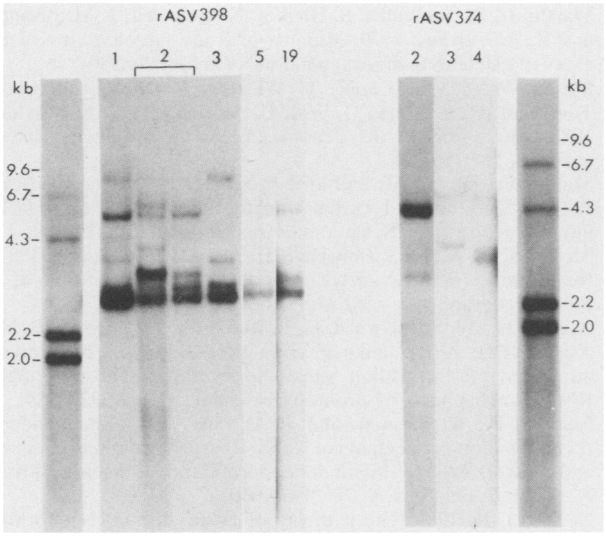

FIG. 14. Effect of helper virus function on the viral RNA patterns of rASV374- and rASV398-infected cells. Details of the experiment are described in the text. Numbers represent individual single transformed colony-derived culture of either rASV398- or rASV374-infected ev^- CEF which had been preinfected with RAV-60. The RNA patterns revealed by either the 5′ probe or the *src* probe are shown for rASV398 and rASV374 clones, respectively.

RSV-, td RSV-, and RAV-60-infected CEF contained a small fraction (up to 10%) of read-through transcripts among the steady-state viral RNAs (S. A. Herman, and J. M. Coffin, personal communication). Subsequent cleavage and polyadenylation nevertheless occurs specifically at a fixed distance from the AAUAAA signal sequence to give rise to uniform RNA species. Specificity of the 3′ cleavage site in those three $env^- pol^-$ rASV RNAs appears to be relaxed and is apparently due to the deletion in *pol*. It is not clear what sequences and factors confer the specificity of the cleavage. Recently, McDevitt et al. (36) identified a 35-nucleotide sequence immediate downstream from the polyadenylation site of the adenovirus E2A gene to be involved in the processing of the 3′ end of E2A mRNA. A downstream deletion extending 15 nucleotides into the 35-nucleotide sequence abolished the ability to produce a functional E2A mRNA.

Preliminary sequence analysis of the LTR region of rASV3812 (unpublished data) revealed only three base changes, in comparison to SR-A (New York) RSV (a TT to AA change and a guanine to adenine change at positions 74 and 173, respectively, from the beginning of U3) (50). However, the published sequences of both SR-A (San Francisco) (48) and PR-C (43) RSV are identical to those of rASV3812 at the corresponding positions described above. Therefore, it is unlikely that these base changes in the U3 region are responsible for the observed aberrant RNA patterns. All the canonical signal sequences for transcription and processing of mRNA were present in the LTR region of rASV3812. Moreover, as mentioned above, insertion of the 3′ *pol* sequence back into the genome of rASV3812 corrected the abnormality of the RNA pattern. This also argues against the involvement of LTR in the aberrant RNA processing observed here. Sequence analysis of the rASV3812 LTR further confirms the correlation of the 3′ *pol* deletion in those rASVs and the abnormal RNA patterns. It is likely that the 3′ *pol* region is required for the specific cleavage of the RSV mRNA via formation of a unique secondary RNA structure recognized by the nuclease. Deletion of the 3′ *pol* sequence would then result in the loss of the specificity of the 3′ cleavage and allow some of the read-through cellular sequences to remain on the mature mRNAs. The length of cellular sequences remaining linked to the viral RNA would depend on the relative strength of the normal and additional cleavage sites in viral and read-through sequences. Therefore, the pattern of viral RNAs in those defective rASVs varied according to the integration sites of provirus. It can be predicted from the above consideration that the primary RNA transcripts of RSV provirus should contain various extents of downstream cellular sequences. However, this may not be easily detected, since cleavage and polyadenylation may precede the termination of transcription (39).

The read-through transcription observed here is distinct from that of promoter insertion observed in the process of leukemogenesis by avian leukosis viruses (24). The latter is a result of the insertion of provirus next to the c-*myc* gene, and the provirus invariably has deleted most of the sequences upstream from the 3′ LTR, thereby leaving only a functional 3′ LTR that promotes the downstream transcription (12, 37, 38, 41). By contrast, the read-through transcription observed here apparently resulted from transcription of an intact provirus. The downstream cellular sequences remained linked to the viral RNAs, presumably only because of the aberration in the 3′ cleavage of primary RNA transcripts in those $env^- pol^-$ rASV-infected cells.

ACKNOWLEDGMENTS

I thank H. Hanafusa for providing the rASV NP clones used in the initial experiments of this study and for his continuous interest and stimulating discussions during the course of this study and comments on the manuscript, C. Grandori for her contribution in part of the proviral DNA analyses, F. Cross for comments on the manuscript, and B. Mayer and B. Edelstein for their excellent technical assistance.

This work was supported by the Public Health Service grants CA18213 and CA29339 from National Cancer Institute. L.-H.W. was a recipient of the Public Health Service Research Career Development Award CA00574 from the National Cancer Institute.

LITERATURE CITED

1. **Astrin, S. M., E. G. Buss, and W. S. Hayward.** 1979. Endogenous viral genes are nonessential in the chicken. Nature (London) **282**:339–334.
2. **Breathnach, R., and P. Chambon.** 1981. Organization and expression of eukaryotic split genes coding for proteins. Annu. Rev. Biochem. **50**:349–383.
3. **Cohen, J. C.** 1980. Methylation of milk-borne and genetically transmitted mouse mammary tumor virus proviral DNA. Cell **19**:653–662.
4. **Cooper, G. M., and L. Silverman.** 1978. Linkage of the endogenous avian leukosis virus genome of virus-producing chicken cells to inhibitory cellular DNA sequences. Cell **15**:573–577.
5. **Cooper, G. M., and H. M. Temin.** 1976. Lack of infectivity of the endogenous avian leukosis virus-related genes in the DNA of uninfected chicken cells. J. Virol. **17**:422–430.
6. **Darlix, J.-L., and P.-F. Spahr.** 1982. Binding sites of viral protein p19 onto Rous sarcoma virus RNA and possible controls of viral functions. J. Mol. Biol. **160**:147–161.
7. **Darnell, J. E., Jr.** 1982. Variety in the level of gene control in eukaryotic cells. Nature (London) **297**:365–371.
8. **Delorbe, W. J., P. A. Luciw, H. M. Goodman, H. E. Varmus, and J. M. Bishop.** 1980. Molecular cloning and characterization of avian sarcoma virus circular DNA molecules. J. Virol. **36:**

50–61.
9. **Ford, J. P., and M.-T. Hsu.** 1978. Transcription pattern of in vitro-labeled late simian virus 40 RNA: equimolar transcription beyond the mRNA 3′ terminus. J. Virol. **28**:795–801.
10. **Fraser, N. W., J. R. Nevins, E. Ziff, and J. E. Darnell, Jr.** 1979. The major late adenovirus type-2 transcription unit: termination is downstream from the last poly(A) site. J. Mol. Biol. **129**:643–656.
11. **Fuhrman, S. A., C. Van Beveren, and I. M. Verma.** 1981. Identification of a RNA polymerase II initiation site in the long terminal repeat of Moloney murine leukemia viral RNA. Proc. Natl. Acad. Sci. U.S.A. **78**:5411–5415.
12. **Fung, Y.-K., A. M. Fadly, L. B. Crittenden, and H.-J. Kung.** 1981. One of the mechanism of retrovirus-induced avian lymphoid leukosis: deletion and integration of the provirus. Proc. Natl. Acad. Sci. U.S.A. **78**:3418–3422.
13. **Gilmartin, G. M., and J. T. Parsons.** 1983. Identification of transcriptional elements within the long terminal repeat of Rous sarcoma virus. Mol. Cell. Biol. **3**:1834–1845.
14. **Guntaka, R. V., P. V. Rao, S. A. Mitsialis, and R. Katz.** 1980. Modification of avian sarcoma proviral DNA sequences in nonpermissive XC cells but not in permissive chicken cells. J. Virol. **34**:569–572.
15. **Hanafusa, H.** 1969. Rapid transformation of cells by Rous sarcoma virus. Proc. Natl. Acad. Sci. U.S.A. **63**:318–325.
16. **Hanafusa, H., and T. Hanafusa.** 1968. Further studies on RSV production from transformed cells. Virology **34**:630–636.
17. **Hanafusa, H., and T. Hanafusa.** 1971. Noninfectious RSV deficient in DNA polymerase. Virology **43**:313–316.
18. **Hanafusa, H., T. Hanafusa, and H. Rubin.** 1963. The defectiveness of Rous sarcoma virus. Proc. Natl. Acad. Sci. U.S.A. **49**:572–582.
19. **Hanafusa, T., H. Hanafusa, and T. Miyamoto.** 1970. Recovery of a new virus from apparently normal chick cells by infection with avian tumor viruses. Proc. Natl. Acad. Sci. U.S.A. **67**: 1797–1803.
20. **Hanafusa, T., H. Hanafusa, T. Miyamoto, and E. Fleissner.** 1972. Existence and expression of tumor virus genes in chick embryo cells. Virology **47**:475–482.
21. **Hanafusa, T., T. Miyamoto, and H. Hanafusa.** 1970. A type of chick embryo cell that fails to support formation of infectious RSV. Virology **40**:55–64.
22. **Haseltine, W. A., D. G. Kleid, A. Panet, E. Rothenberg, and D. Baltimore.** 1976. Ordered transcription of RNA tumor virus genomes. J. Mol. Biol. **106**:109–131.
23. **Hayward, W. S.** 1977. Size and genetic content of viral RNAs in avian oncovirus-infected cells. J. Virol. **24**:47–63.
24. **Hayward, W. S., B. G. Neel, and S. Astrin.** 1981. Activation of a cellular gene by promoter insertion in ALV-induced lymphoid leukosis. Nature (London) **290**:475–480.
25. **Hofer, E., and J. E. Darnell, Jr.** 1981. The primary transcription unit of the mouse β-major globin gene. Cell **23**:585–593.
26. **Humphries, E. H., C. Glover, R. A. Weiss, and J. R. Arrand.** 1979. Differences between the endogenous and exogenous DNA sequences of Rous-associated virus-0. Cell **18**:803–815.
27. **Jaenisch, R.** 1983. Endogenous retroviruses. Cell **32**:5–6.
28. **Ju, G., and A. M. Skalka.** 1980. Nucleotide sequence analysis of the long terminal repeat (LTR) of avian retroviruses: structural similarities with transposable elements. Cell **22**:379–386.
29. **Kawai, S., and H. Hanafusa.** 1973. Isolation of defective mutant of avian sarcoma virus. Proc. Natl. Acad. Sci. U.S.A. **70**: 3493–3497.
30. **Leis, J. P., P. Scheible, and R. E. Smith.** 1980. Correlation of RNA binding affinity of avian oncornavirus p19 proteins with the extent of processing of viral genome RNA in cells. J. Virol. **35**:722–731.
31. **Lerner, T. L., A. M. Skalka, and H. Hanafusa.** 1981. Integration of Rous sarcoma virus DNA into chicken embryo fibroblasts: no preferred proviral acceptor site in the DNA of clones of singly infected transformed chicken cells. J. Virol. **40**:421–430.
32. **Linial, M., and W. S. Mason.** 1973. Characterization of two conditional early mutants of Rous sarcoma virus. Virology **53**:258–273.
33. **Martin, G. S., K. Radke, S. Hughes, N. Quintrell, J. M. Bishop, and H. E. Varmus.** 1979. Mutants of Rous sarcoma virus with extensive deletions of viral genome. Virology **96**:530–546.
34. **Mason, W. S., M. Linial, T. W. Hsu, R. N. Eisenman, J. Townsend, G. E. Mark, G. Seal, C. Aldrich, and J. M. Taylor.** 1982. Alterations in the genomes of avian sarcoma viruses. Virology **117**:456–474.
35. **Mathey-Prevot, B., M. Shibuya, J. Samarut, and H. Hanafusa.** 1984. Revertants and partial transformants of rat fibroblasts infected with Fujinami sarcoma virus. J. Virol. **50**:325–334.
36. **McDevitt, M. A., M. J. Imperiale, H. Ali, and J. R. Nevins.** 1984. Requirement of a downstream sequence for generation of a poly(A) addition site. Cell **37**:993–999.
37. **Neel, B. G., W. S. Hayward, H. L. Robinson, J. Fang, and S. M. Astrin.** 1981. Avian leukosis virus-induced tumors have common proviral integration sites and synthesize discrete new RNAs: oncogenesis by promoter insertion. Cell **23**:323–334.
38. **Neiman, P., K. Beemon, and J. A. Luce.** 1981. Independent recombination between avian leukosis virus terminal sequences and host DNA in virus-induced proliferative disease. Proc. Natl. Acad. Sci. U.S.A. **78**:1896–1900.
39. **Nevins, J. R.** 1983. The pathway of eukaryotic mRNA formation. Annu. Rev. Biochem. **52**:441–446.
40. **Nevins, J. R., and J. E. Darnell, Jr.** 1978. Steps in the processing of Ad2 mRNA: poly(A)$^+$ nuclear sequences are conserved and poly(A) addition precedes splicing. Cell **15**:1477–1493.
41. **Payne, G. S., S. A. Courtneidge, L. B. Crittenden, A. M. Fadly, J. M. Bishop, and H. E. Varmus.** 1981. Analysis of avian leukosis virus DNA and RNA in bursal tumors: viral gene expression is not required for maintenance of tumor state. Cell **23**:311–322.
42. **Saule, S., A. Sergeant, G. Torpier, M. B. Raes, S. Pfeifer, and D. Stehelin.** 1982. Subgenomic mRNA in OK10 defective leukemia virus-transformed cells. J. Virol. **42**:71–82.
43. **Schwartz, D. E., R. Tizard, and W. Gilbert.** 1983. Nucleotide sequence of Rous sarcoma virus. Cell **32**:853–869.
44. **Sawyer, R. C., C. W. Rettenmier, and H. Hanafusa.** 1979. Formation of Rous associated virus-60: origin of the polymerase gene. J. Virol. **29**:856–862.
45. **Shibuya, M., L.-H. Wang, and H. Hanafusa.** 1982. Molecular cloning of Fujinami sarcoma virus genome and its comparison with sequences of other related transforming viruses. J. Virol. **42**:1007–1016.
46. **Southern, E. M.** 1975. Detection of specific sequences among DNA fragments separated by gel electrophoresis. J. Mol. Biol. **98**:503–517.
47. **Stuhlman, H., D. Jahner, and R. Jaenisch.** 1981. Infectivity and methylation of retroviral genomes is correlated with expression in the animal. Cell **26**:221–232.
48. **Swanstrom, R., W. J. Delorbe, J. M. Bishop, and H. E. Varmus.** 1981. Nucleotide sequence of cloned unintegrated avian sarcoma virus DNA: viral DNA contains direct and inverted repeats similar to those in transposable elements. Proc. Natl. Acad. Sci. U.S.A. **78**:124–128.
49. **Swanstrom, R., R. C. Parker, H. E. Varmus, and J. M. Bishop.** 1983. Transduction of a cellular oncogene: the genesis of Rous sarcoma virus. Proc. Natl. Acad. Sci. U.S.A. **80**:2519–2523.
50. **Takeya, T., R. A. Feldman, and H. Hanafusa.** 1982. DNA sequence of the viral and cellular *src* gene of chickens. I. Complete nucleotide sequence of an *Eco*RI fragment of recovered avian sarcoma virus which codes for gp37 and pp60^{src}. J. Virol. **44**:1–11.
51. **Thomas, P. S.** 1980. Hybridization of denatured RNA and small DNA fragments transferred to nitrocellulose. Proc. Natl. Acad. Sci. U.S.A. **70**:5201–5205.
52. **Wang, L.-H., M. Beckson, S. M. Anderson, and H. Hanafusa.** 1984. Identification of the viral sequence required for the generation of recovered avian sarcoma viruses and characterization of a series of replication-defective recovered avian sarcoma viruses. J. Virol. **49**:881–891.
53. **Wang, L.-H., and P. Duesberg.** 1974. Properties and location of poly(A) in Rous sarcoma virus RNA. J. Virol. **14**:1515–1529.
54. **Wang, L.-H., B. Edelstein, and B. J. Mayer.** 1984. Induction of

tumors and generation of recovered sarcoma viruses by, and mapping of deletions in, two molecularly cloned *src* deletion mutants. J. Virol. **50**:904–913.

55. **Wang, L.-H., R. Feldman, M. Shibuya, H. Hanafusa, M. F. D. Notter, and P. C. Balduzzi.** 1981. Genetic structure, transforming sequence, and gene product of avian sarcoma virus UR1. J. Virol. **40**:258–267.
56. **Wang, L.-H., C. C. Halpern, M. Nadel, and H. Hanafusa.** 1978. Recombination between viral and cellular sequences generated transforming sarcoma virus. Proc. Natl. Acad. Sci. U.S.A. **75**:5812–5816.
57. **Yamamoto, T., B. de Crombrugghe, and I. Pastan.** 1980. Identification of a functional promoter in the long terminal repeat of Rous sarcoma virus. Cell **22**:787–797.
58. **Ziff, E. B.** 1980. Transcription and RNA processing by the RNA tumor viruses. Nature (London) **287**:491–499.